Interfacial water and micro-heterogeneity in aqueous solutions of ionic liquids

Cettina Bottari[1], Láaszlóo Almáasy[2], Barbara Rossi[1], Brenda Bracco[3], Marco Paolantoni[3]*, Andrea Mele[4]*

[1] Elettra Sincrotrone Trieste, S.S. 114 km 163.5, Basovizza, 34149, Trieste, Italy
[2] Institute for Energy Security and Environmental Safety, Centre for Energy Research, Konkoly-Thege Miklós út 29–33, 1121 Budapest, Hungary
[3] Department of Chemistry, Biology and Biotechnology, University of Perugia, Via Elce di Sotto 8, 06123 Perugia, Italy
[4] Department of Chemistry, Materials and Chemical Engineering "G. Natta", Politecnico di Milano, Milano, Italy

*marco.paolantoni@unipg.it, *andrea.mele@polimi.it

Abstract

In this work aqueous solutions of two prototypical ionic liquids (ILs), [BMIM][BF_4] and [BMIM][TfO], were investigated by UV Raman spectroscopy and Small Angles Neutron Scattering (SANS) in the water-rich domain, where strong heterogeneities at mesoscopic length scales (micro-heterogeneity) were expected. Analyzing Raman data by a differential method, the solute-correlated (SC) spectrum was extracted from the OH stretching profiles, emphasizing specific hydration features of the anions. In particular, SC-UV Raman spectra pointed out the molecular structuring of the *interfacial water* in these micro-heterogenous IL/water mixtures, in which IL aggregates coexist with bulk water domains. The organization of the *interfacial water* differs for the [BMIM][BF_4] and [BMIM][TfO] solutions, being affected by specific anion-water interactions. In particular, in the case of [BMIM][BF_4], which forms weaker H-bonds with water, aggregation properties clearly depend on concentration, as reflected by local changes of the *interfacial water*. On the other hand, stronger water-anion hydrogen bonds and more persistent hydration layers were observed for [BMIM][TfO], which likely prevent changes on IL aggregates. The modelling of SANS profiles, extended to [BPy][BF_4] and [BPy][TfO], evidences the occurrence of significant concentration fluctuations for all the systems: this appears as a rather general phenomenon that can be ascribed to the occurrence of IL aggregation, mainly induced by (cation-driven) hydrophobic interactions. Nevertheless, larger concentration fluctuations were observed for [BMIM][BF_4], suggesting that anion-water interactions are relevant in modulating the micro-heterogeneity of the mixture.

Keywords: ionic liquids, interfacial water, micro-heterogeneity, Small Angles Neutron Scattering, UV Raman spectroscopy

INTRODUCTION

The well-known capability of imidazolium-based, aprotic ionic liquids (AILs) to generate polar and non-polar domains is the major source of the structural heterogeneities commonly seen as a fingerprint of these systems [S. M. Urahata, M. C. C. Ribeiro, J. Chem. Phys. 120, 1855–1863 (2004); Y. Wang, G. A. Voth, J. Am. Chem. Soc. 127, 12192–12193 (2005); J. N. A. C. Lopes, A. A. H. Pa`dua, J. Phys. Chem. B 110, 3330–3335 (2006); A. Triolo, O. Russina, H. J. Bleif, E. D. Cola, J. Phys. Chem. B 111, 4641–4644 (2007); Russina et al. J. Phys. Chem. Lett. 3, 27-33 (2012)[1–5]. Such a characteristic behavior, also shared by piperidinium-based AILs [A. Triolo et al. J. Chem. Phys. 130, 164521 (2009)[6]] stems from the interplay between long-range Coulombic interactions and short-range H-bonding, van der Waals and solvophobic ones [Wang, Fayer Chem Rev 120, 5798 (2020)[7]]. Commonly, the extent of heterogeneous organization increases with increasing the length of the cation alkyl chains, due to the enhancement of hydrophobic effects that favors the separation of polar and apolar regions [Wang, Fayer Chem Rev 120, 5798 (2020)[7]].

Water addition can drastically change the inhomogeneous organization of the ILs and, in turn, their macroscopic properties, thus representing a suitable way to tune their behavior in view of specific applications [Y. Kohno, Y. Deguchi, and H. Ohno, Chem. Commun., 48, 7119-7130 (2012); V.A. Azov et al. Chem. Soc. Rev., 47, 1250 (2018); C. Ma et al. Chem. Soc. Rev., 47, 8685 (2018) [8–10]]. At low hydration levels, the nano-domain structuring on ILs is largely maintained, being water molecules dispensed into the polar regions of the IL network, interacting preferentially with the ionic moieties. [V.A. Azov et al. Chem. Soc. Rev., 47, 1250 (2018); Wang, Fayer Chem Rev 120, 5798 (2020)].[7,9] Increasing water concentration favors water clustering, with possible formation of specific architectures such as interconnected water channels, confined water domains or reverse micelles, depending on the IL nature and concentration [A. Azov et al. Chem. Soc. Rev., 47, 1250 (2018), Moreno et al. J. Phys Chem. 112, 7826 (2008)[9,11]]. At higher water contents, generally corresponding to water mole fractions $x_w > 0.9$, water molecules produce extended percolating networks, within which IL species self-organize based on their polar/apolar character [Wang, Fayer Chem Rev 120, 5798 (2020)[7]] The formation of a bi-continuous structure of interpenetrating percolating networks of both water and IL was also considered [Nordness and Brenneckeke, Chem Rev 120, 12873 (2020)[12]]. In this water-rich domain, IL/water mixtures can exhibit enhanced spatial (and dynamical) heterogeneities, also due to the possible formation of specific IL aggregates (i.e. micellar-like) dispersed in the aqueous medium [Wang, Fayer Chem Rev 120, 5798 (2020); V.A. Azov et al. Chem. Soc. Rev[7,9]]. Commonly, the dissociation of ILs in small ion clusters requires larger water contents, starting from $x_w \sim 0.95$ [Nordness and Brenneckeke, Chem Rev 120, 12873 (2020)[12]], yet ion-pairs are expected to exist even in more diluted conditions [Ma et al. Chem. Soc. Rev., 47, 8685 (2018)[10]].

Crucial information on the heterogeneities of IL/water mixtures was ~~can be~~ obtained by Small Angle Neutron Scattering (SANS) experiments on prototypical aqueous solutions of [BMIM][BF_4] [Gao and Wagner Langmuir 32, 5078–5084 (2016)][13] Bowers et al. [Bowers et al. Langmuir 20, 2191–2198 (2004)][14], from SANS, surface tension and conductivity measurements, suggested that starting from diluted conditions, polydisperse spherical [BMIM][BF_4] aggregates form above a critical aggregation concentration (CAC), located at around IL mole fraction $x_{IL} \sim 0.015$ ($x_w \sim 0.985$). Koga et al. analyzing thermodynamic data identified a transition in the "solution structure" just at $x_{IL} = 0.015$, which was related to the begin of either direct or water-mediated ion association [Kataynagi et al. JPCB 108, 19451–19457 (2004)[15]]. A subsequent work of Almasy et al. [Almasy et al. JPCB 112, 2382–2387 (2008)[16]] demonstrated that the SANS profiles of [BMIM][BF_4]/water mixtures can be well interpreted in terms of strong concentration fluctuations within the range $0.02 < x_{IL} < 0.16$ and that the greatest heterogenous structuring occurs at $x_{IL} \sim 0.075$ (about 50 % in volume), when the system approaches the phase separation. It was also remarked how the formation of micellar-like aggregates could not be

excluded nor confirmed, due to the dominant scattering contribution arising from concentration fluctuations [Almasy et al. JPCB 112, 2382–2387 (2008)[16]]. Analogous heterogeneous mixing was observed in other binary organic solvent/water and IL/organic solvent mixtures [Perera et al. JCP 123, 024503 (2005); Almasy et el., Fluid Phase Equilibria 257, 114-119, 2007; Shimomura, Takamuku PCCP 12, 12316 (2010) [17-19]]. On the other hand, according to the SANS study of Kusano et al. [Kusano et al. J Sol Chem 42, 1888–1901 (2013)[20]], [BMIM][Cl] and [BMIM][Br] mix homogenously with water, due to the strong hydration capability of the anions. Remarkably, in the case [BMIM][NO_3]/water mixture, SANS experiments indicated the presence of confined water within the IL network - referred to as "water pockets" (WP) - starting from rather diluted conditions $x_{IL}\sim 0.05$ to about $x_{IL}\sim 0.30$ [Abe et al. JPCL 5, 1175–1180 (2014)[21]], further evidencing that, even for relatively small cations, a variety of organization features might exist in the water-rich domain. Concerning the aggregation of pyridinium-based ILs in water, clear signatures of interparticle interactions were not observed by SANS experiments for 1-butylpyrinidium and 1-hexylpyridinium chlorides, while a distinct structural peak was observed for longer chain cations [Sastry et al. J. Colloid and Interface Science 371, 52–61 (2012)[22]].

The full concentration range of [BMIM][BF_4]/water mixtures was explored by Gao and Wagner [Gao and Wagner Langmuir 32, 5078–5084 (2016)[14]] based on SANS and literature results. It was argued that water molecules remain dispersed within the IL network up to $x_w\sim 0.7$ ($x_{IL}\sim 0.3$), while for higher x_w values a microphase separation would take place, due to the formation of water nano-clusters among the percolating IL network. These water pockets progressively grow with further water addition and a phase inversion will occur for $x_w > 0.84$ ($x_{IL} < 0.16$) due to the formation of micelle-like IL aggregates, dispersed in the percolating network of water. Additionally, the full dissociation of IL species would occur only for water mole fractions larger than $x_w\sim 0.985$ ($x_{IL}\sim 0.015$), as suggested by Koga et al. (Kataynagi et al. JPCB 108, 19451–19457 (2004)[15]]. To note that mixtures in which salt/water ratios are larger than one by volume ($x_{IL} > 0.075$ for [BMIM][BF_4]), were recently conceptualized as a promising class of systems in different application areas and specifically denoted as "water-in-salt" mixtures [A. Azov et al. Chem. Soc. Rev., 47, 1250 (2018)[9]]. It has been suggested that the water structuring in BMIM-based IL mixtures might be tuned by changing the nature of the anion, which also determines the IL hydrophilic/hydrophobic character and its full miscibility with water [McDaniel et al. J. Phys. Chem. B 2019, 123, 5343−5356; A. Verma et al. Int. J. Mol. Sci. **2020**, 21, 403[23,24]]. In particular, while [BMIM][BF_4] and [BMIM][TfO] are hydrophilic and full miscible with water [McDaniel et al. J. Phys. Chem. B 2019, 123, 5343−5356; A. Verma et al. Int. J. Mol. Sci. **2020**, 21, 403[23,24]], the replacement of BF_4^- with TfO^- would make the system more hydrophobic, promoting water percolation. Overall, specific aggregation properties of AIL/water mixtures formed by short-chain cations, strongly depend on anion type and water contents, and are still under debate.

The mesoscopic picture on IL/water mixtures derived by SANS experiments, can be flanked by an atomistic point of view on their intermolecular interactions achieved by vibrational spectroscopies, [Paschoal, Faria, Riberio Chem Rev 117, 7053–712 (2017)[25] as they are sensitive to modulations of local potentials around a probing oscillator. Regarding the prototypical [BMIM][BF_4]/water system, Fazio et al. [Fazio et al. J. Raman Spectr. 39, 233–237 (2008)[26]], showed that a fraction of bulk-like water in the mixture grows up from $x_w\sim 0.5$ and it starts to affect anion-cation interaction at $x_w\sim 0.7$. The vibrational study of Jeon et al. [Jeon et al. JPCB 112, 923–928 (2008)[27]], suggested the occurrence of structural changes in the water-rich domain, at around $x_w\sim 0.93$ and 0.98, as inferred from the concentration dependence of the signals of the anion, cation and water as well. It was proposed that cation aggregation (or micellization) occurs at $x_{IL} > 0.02$ ($x_w < 0.98$), leading to modifications of the water structuring. Indeed, MD simulations indicate that IL aggregation takes place at $x_w > 0.8$, attaining its maximum extent at $x_w \sim 0.9$-0.95 [Zhong et al. JPCB 116, 3249–3263 (2012)[28]]. On the other hand, analyzing the OD stretching band in the IR spectrum of [BMIM][BF_4]/D_2O mixtures, Zheng et al. [Zheng et al. Spectroc. Acta Part A 226, 117624 (2020)[29]] suggested that IL aggregates and ion pairs dissociate

when x_w > 0.9. As a representative case of pyridinium-based IL, aqueous mixtures of 1-butylpyridinium tetrafluoroborate ([BPy][BF_4]) were studied by the combined use of IR and DFT methods by Wang et al. [Wang et al. JPCB 114, 8689 (2010)[30]]. These authors inferred that the substitution of BMIM with BPy would impact the overall H-bonding of the mixtures, basically due to the different acidity and steric hindrance of the aromatic C-H groups in the two cations.

We remark that the characteristic spectral features of the OH stretching of water molecules dispersed within concentrated ILs, can be observed by vibrational spectroscopies [Cammarata et al. PCCP 3, 5192 (2001); Koddermann, Ludwig Angew. Chem. Int. Ed. 45, 3697 (2006) Yoshimura et al. J Mol Liq 286, 110874 (2019) [31–33]]. In these conditions the spectral features were commonly related to water-anion interactions, albeit some discrepancies on the specific geometry of the clusters persist [Zheng et al. Spectroc. Acta Part A 226, 117624 (2020); Cammarata et al. PCCP 3, 5192 (2001); Yoshimura et al. J Mol Liq 286, 110874 (2019) [29,31,33]]. Nevertheless, drawing a clear picture of the water state in the water-rich concentration range (x_w> 0.8) is much more challenging, as hydrating water molecules coexist with bulk-like ones and the OH stretching band broadens significantly, encompassing water-water and water-IL contributions. Considering the micro-heterogenous character of the system, this hydration water can be conjectured as a sort of "micro-interface", separating bulk water and IL-rich domains, with features related to IL clustering and/or concentration fluctuations, which would depend on the IL content. Thus, gaining insights on this *interfacial water* appears crucial for a molecular-level understanding of the physicochemical and solvation properties of the mixtures, but difficult to achieve.

Here, AILs/water systems were investigated in the water-rich regime, when IL and water mesoscopic domains are expected to form. Aqueous solutions of [BMIM][BF_4], [BMIM][TfO] were analyzed by SANS and UV Raman spectroscopy to relate their micro-heterogenous character with the molecular state of water at the "micro-interface". The SANS investigation was further extended to [BPy][BF_4] and [BPy][TfO]/water mixtures to highlight the effects induced by the cation on the micro-heterogeneous mixing. The atomistic view was derived by UV-Raman experiments, based on the approach proposed by Ben-Amotz et al. [Ben-amotz et al, J. Am. Chem. Soc. 2008, 130, 14, 4576–4577; Ben-Amotz J. Am. Chem. Soc. 2019, 141, 27, 10569–10580; [34,35]]. The method, when coupled with multivariate curve resolution (MCR) analysis, was proven suitable to isolate from the OH stretching Raman band of water the so-called solute-correlated spectrum (SC), which contains the spectral contribution of those water molecules affected by the solute (hydrating water) [Ben-amotz et al, J. Am. Chem. Soc. 2008, 130, 14, 4576–4577; Ben-Amotz J. Am. Chem. Soc. 2019, 141, 27, 10569–10580; Fega *Appl Spectrosc* **66**, 282–288 (2012); Davis *Nature* **491**, 582–585 (2012); Wilcox *Faraday Discuss.* 2013, *167*, 177[34-38]]. Here, UV-Raman SC spectra were obtained by a direct spectral subtraction procedure [Ben-Amotz J. Am. Chem. Soc. 2019, 141, 27, 10569–10580; Fega *Appl Spectrosc* **66**, 282–288 (2012); Wilcox *Faraday Discuss.* 2013, *167*, 177[35,36,38]], providing novel molecular insights on the *interfacial water* in micro-heterogenous IL/water mixtures.

MATERIALS AND METHODS

Preparation of ionic liquids/water solutions

1-butyl-3-methylimidazolium tetrafluoroborate ([BMIM][BF_4]), 1-butyl-3-methylimidazolium triflate ([BMIM][TfO]), 1-butylpyridinium tetrafluoroborate ([BPy][BF_4]) and 1-butylpyridinium triflate([BPy][TfO]) were purchased from IoLiTec with a purity of 99%. The molecular structures of the components of ILs are displayed in Scheme 1. For UV Raman experiments, ILs/water solutions were prepared using high-purity water deionized through a MilliQ^{TM} water system (>18 M cm resistivity). Heavy water of 99.3 atom % deuterium content was used for preparing the solutions for SANS experiments, to increase the contrast in the scattering length densities between IL and water, thus

improving the experimental accuracy. The aqueous solutions of ILs were prepared at different IL mole fractions, $x_{IL} = \frac{n_{IL}}{n_{IL}+n_{water}}$, where n_{IL} and n_{water} are the number of moles of IL and water, respectively.

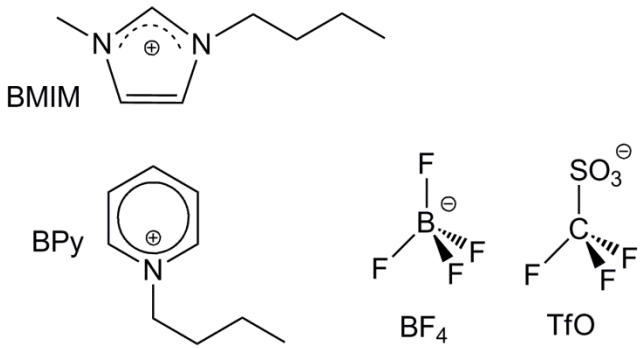

Scheme 1. Molecular formulae and labels of the cationic and an ionic components of the examined ILs.

SANS measurements

SANS experiments were carried out using the *Yellow Submarine* diffractometer operating at the Budapest Neutron Center [Almasy L., J. Surf. Investig. 15, 527-531 , 2021][39]. Samples were placed in 2 mm-thick Hellma quartz cells. Temperature was controlled within 0.1 K using a Julabo FP50 water circulation thermostate. The range of scattering vectors q was set to 0.038-0.38 Å^{-1}. The q value is defined as $q = 4\pi/\lambda \sin\theta$ where 2θ is the scattering angle. In order to have access to the whole range of q, we used two different configurations with sample-detector distances 1.15 and 5.125 m and the incident neutron wavelength was set to 4.4 Å.

The raw data have been corrected for sample transmission, scattering from empty cell, and room background. Correction to the detector efficiency and conversion of the measured scattering to absolute scale was performed by normalizing the spectra to the scattering from a light water sample.

UV Raman measurements

UV Raman experiments were carried out by exploiting the synchrotron-based UV Raman set-up available at the BL10.2-IUVS beamline of Elettra Sincrotrone Trieste (Italy) [ref libro IUVS][40]. The Raman spectra of ILs/water solutions were recorded using excitation wavelengths in the deep UV range at 248 and 266 nm. These excitation conditions were chosen in order to obtain suitable Raman signals of the ILs, even at the higher dilution considered, minimizing the fluorescence background and with the best features in terms of the spectral resolution and signal-to-noise ratio. The 248 nm excitation wavelength, provided by the synchrotron source (SR), was set by regulating the undulator gap and using a Czerny–Turner monochromator (Acton SP2750, Princeton Instruments, Acton, MA, USA) equipped with a holographic grating with 1800 grooves per mm for monochromatizing the incoming SR. The excitation radiation at 266 nm was provided by a CryLas FQSS 266-Q2 diode pumped passively Q196 switched solid-state laser. The UV Raman spectra were collected in back-scattered geometry using a single pass of a Czerny–Turner spectrometer (Trivista 557, Princeton Instruments, 750 mm focal length) and detected with a CCD camera. The spectral resolution was set at 1.6 and 2 cm^{-1}/pixel for the measurements with 266 and 248 nm as excitation wavelengths, respectively. The calibration of the spectrometer was standardized using cyclohexane (spectroscopic grade, Sigma Aldrich). The power of the beam on the sample was measured to be of few µW; any possible photo-damage effect due to prolonged exposure of the sample to UV radiation was avoided by continuously spinning the sample cell during the measurements. Solute-correlated (SC) spectra [Ben-amotz et al, J. Am. Chem. Soc. 2008, 130, 14, 4576–

4577[34,35] were extracted from the OH stretching distribution by a direct spectral subtraction procedure, as the difference between the spectrum of the mixture and a properly rescaled spectrum of neat water. The rescaling factor is determined in such a way that the resulting difference distribution is non-negative and with the minimum area (Wilcox et al, Faraday Discuss., 2013, 167, 177-190[38]).

RESULTS AND DISCUSSION

This section is structured in two parts: in the first part, hydration and aggregation properties in AIL/water mixtures will be investigated at the length scale of the chemical bonds by UV Raman spectroscopy, taking [BMIM][BF_4] and [BMIM][TfO] as a paradigm. The second part will explore structural features at the mesoscopic length scale as derived by SANS experiments, in the light of the solvation picture derived from UV Raman experiments.

The microscopic viewpoint: UV Raman experiments. Water-rich mixtures of [BMIM][BF_4] and [BMIM][TfO] were examined as a function of concentrations ($0.02<x_{IL}<0.16$) by UV Raman spectroscopy, focusing on the OH stretching spectral region (3000-3800 cm^{-1}), which is particularly sensitive to the H-bonding configurations of water [Gallina, et al. J. Phys. Chem. B 110, 8856 (2006); Paolantoni, et al. J. Phys. Chem. A 113, 15100 (2009); C. Bottari et al. J. Raman. Spec., 49, 1076-1085 (2018)[41–43]]. Several IR and Raman studies have been already performed to characterize these mixtures [Fazio et al. J. Raman Spectrosc. 2008; 39: 233–237; Cammarata et al. PCCP 3, 5192 (2001); Yoshimura et al. J Mol Liq 286, 110874 (2019); Masaki, Shirota et al. J. Phys. Chem. B, 114, 6323 (2010); Pastor et al, J. Phys. Chem. B, 110, 10896-10902, 2006; [26,31,33,44,45]] however a clear description of the hydration properties of the two systems in the presence of a large amount of water ($x_w> 0.8$) is still missing.

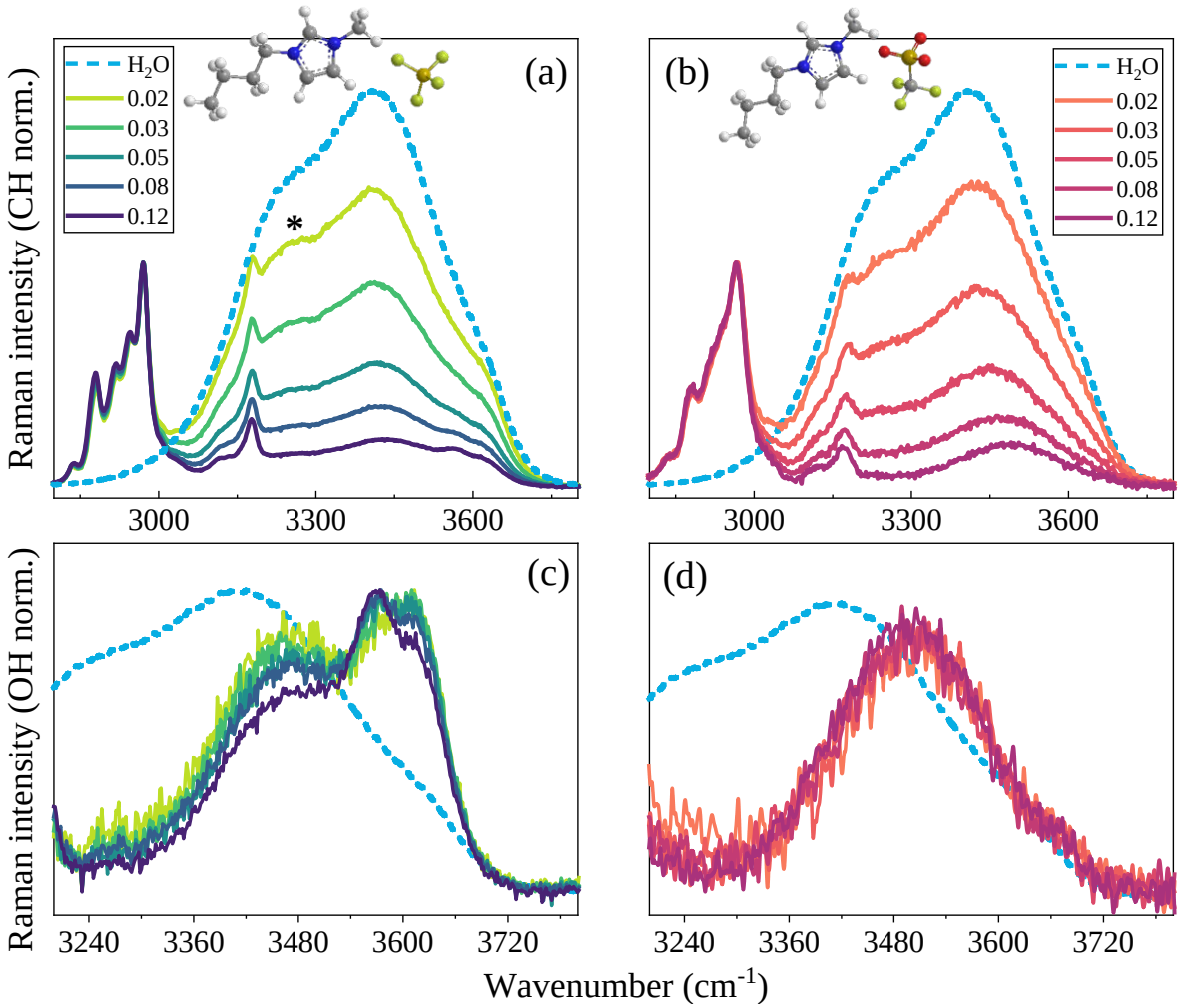

Figure 1. UV Raman spectra of [BMIM][BF_4] (a) and [BMIM][TFO] (b) aqueous solutions at different IL mole ratio, normalized on CH stretching signals (2800-3000 cm^{-1}); the spectrum of neat water is reported in the same graphs (dot line). The symbol * marks the spectral signature at around 3200 cm^{-1}, due to the ice-like component of bulk water. Solute correlated (SC) UV Raman spectra obtained for [BMIM][BF_4] (c) and [BMIM][TFO] (d), after rescaling on the maximum intensity; the Raman spectrum of neat water is shown in the same panels (dot line).

The Raman spectra (2800-3800 cm^{-1}) for the [BMIM][BF_4] and the [BMIM][TfO] aqueous solutions are reported in Figure 1(a) and (b), respectively, together with the spectrum of pure water. The spectra of the mixtures were normalized on the CH stretching signals (2800-3000 cm^{-1}), while the spectrum of pure water was arbitrarily rescaled, for comparative purposes. For both systems (Figure 1(a), 1(b)), the broad OH stretching band (3000-3800 cm^{-1}) shows a decrease in intensity and a global shift towards higher wavenumbers with the increase of IL content. This blue-shift indicates the general weakening of the H-bond interactions and destructuring of the H-bond network typical of water, [Paolantoni, et al. J. Phys. Chem. A 113, 15100 (2009)[42]] owing to the substitution of water-water H-bonds with specific water-anion ones. Modifications of the OH stretching band are mainly ascribed to changes of the H-bonding state of water acting as H-donor, due to the establishment of new O-H···X interactions with the anions [Masaki, Shirota et al. J. Phys. Chem. B, 114, 6323 (2010)[44]]. To note that water-anion H-bonds are expected to be relevant even at high IL contents, when water-cation correlations become less significant [Zhong, Cao et al. JCPB, 116, 3249-3263, 2012; Schroder, et al. JPC, 129,184501, 2008 [28,46]].

Specific information about the "interfacial water" were extracted from the solute-correlated spectra (SC) by a direct spectral subtraction procedure, considering the spectrum of pure water as reference for

the bulk water in the mixture [Ben-Amotz et al, J. Am. Chem. Soc. 2008, 130, 14, 4576–4577; Wilcox et al. *Faraday Discuss.* **167**, 177 (2013).[34,38]]. The resulting SC-UV Raman spectra were compared in Figure 1(c) and 1(d) for the [BMIM][BF_4] and [BMIM][TfO] solutions, respectively, and after normalization to the maximum intensity. The SC-UV Raman spectra emphasize the (minimum) perturbation on the water structure as induced by the solute [Ben-Amotz et al, J. Am. Chem. Soc. 2008, 130, 14, 4576–4577; Wilcox et al. *Faraday Discuss.* **167**, 177 (2013).[34-38]]. We remark that in the reported spectral region (3240 – 3720 cm^{-1}) no direct spectral contributions arising from the cation and anion are present. For both systems, the SC spectra are located at higher wavenumbers compared to the spectrum of pure water, confirming that, under the influence of the anions, hydrating water molecules form weaker H-bonds than in the bulk.

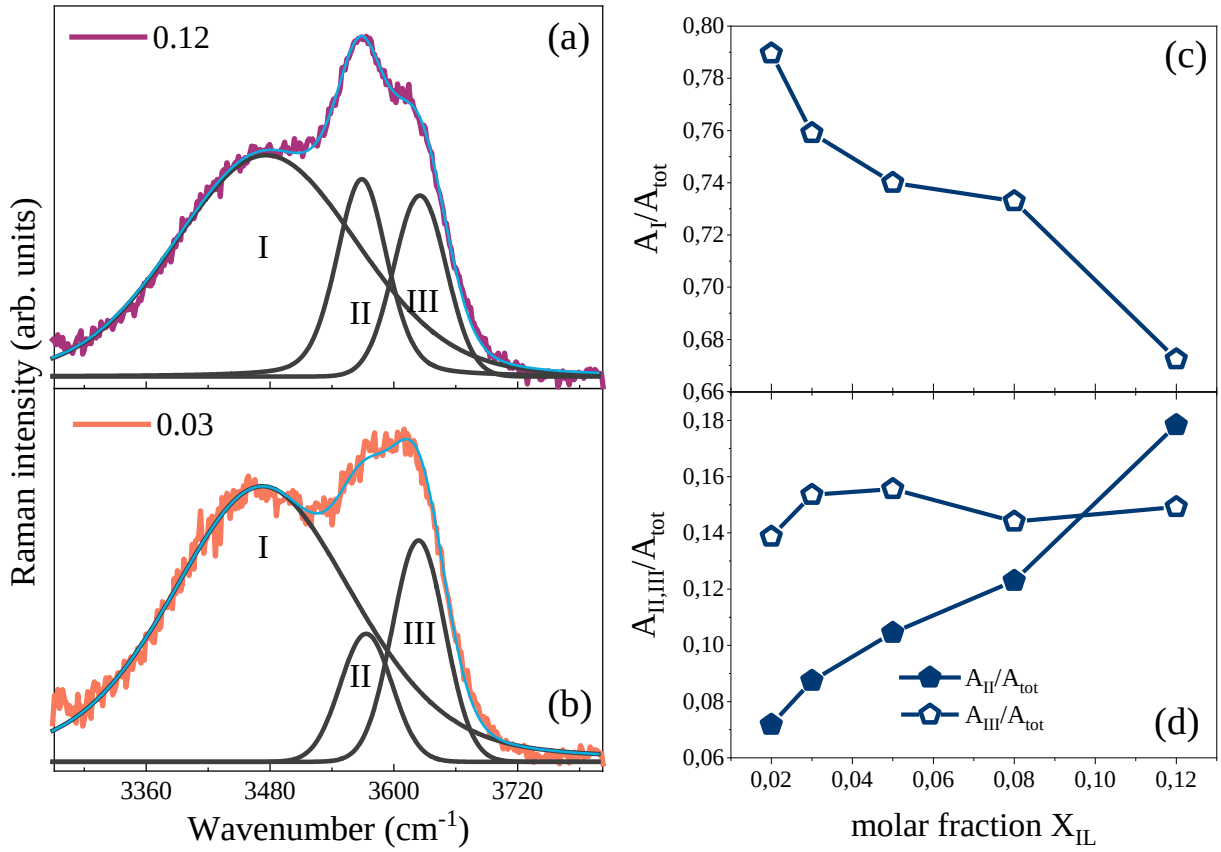

Figure 2. The results of a fitting procedure using three Voigt functions to reproduce the SC-UV Raman spectra of [BMIM][BF_4] solutions at two representative concentrations: X_{IL}= 0.12 (a) and X_{IL}= 0.03 (b). The relative peak areas A_I/A_{tot}, A_{II}/A_{tot}, A_{III}/A_{tot} corresponding to component I, II and III, respectively, (normalized to the total area A_{tot}) is also reported as a function of X_{IL} (c)-(d).

The SC spectra of [BMIM][BF_4] solutions (Figure 1(c)) clearly show the presence of different sub-components, whose intensity strongly depend on concentration. Thus, a partial redistribution of different types of water-anion contacts is taking place in the explored concentration domain. The resulting SC spectra can be reproduced by means of a curve-fitting procedure, using three components located at ~3475, 3565 and 3625 cm^{-1}, here referred to as component I, II and III, respectively. The results of the spectral decomposition are reported in Figure 2 (a)-(b) for two representative samples (x_{IL}=0.03 and x_{IL} =0.12). The two high frequency components II and III relate to water molecules involved

in the formation of rather weak H-bonds with BF_4 anions [Cammarata et al. PCCP 3, 5192 (2001); Masaki, Shirota et al. J. Phys. Chem. B, 114, 6323 (2010)[31,44]]. The Raman spectra of water dispersed into concentrated [BMIM][BF_4] samples show two bands at 3565 and 3643 cm^{-1} due to the symmetric ν_1 and asymmetric ν_3 stretching vibrations, respectively [Danten et al. J. Phys. Chem. A, 113, 2873-2889, 2009[47]]. These have been assigned to water molecules interacting with two different anions (A^-), leading to the formation of a "symmetric" adduct ($A^-\cdots H-O-H\cdots A^-$) with two nearly equivalent H-bonds [Danten et al. J. Phys. Chem. A, 113, 2873-2889, 2009[47]]. In the Raman spectrum, the symmetric ν_1 band is significantly more intense than the asymmetric one ν_3, with an intensity ratio of $I\nu_1/I\nu_3$ ~5.6; an opposite situation occurs for the IR spectrum: $I\nu_1/I\nu_3$ ~0.5. [Cammarata et al. PCCP, 3, 5292-5200, 2001; Danten et al. J. Phys. Chem. A, 113, 2873-2889, 2009[31,47]]. Thus, based on their positions and relative intensities in our SC-Raman spectra, component II (~3565 cm^{-1}) can be attributed to the ν_1 mode of the mentioned "symmetric" water configuration, characterized by an H-bonding energy of about 9.5 kJ/mol [Cammarata et al. PCCP, 3, 5292-5200, 2001[31]]. These results demonstrate that the water structures ($A^-\cdots H-O-H\cdots A^-$), previously detected at low water concentrations [Cammarata et al. PCCP, 3, 5292-5200, 2001[31]], continue to exist also in the water-rich domain (Fig 2 (c)) when IL aggregates are dispersed in the aqueous medium [Gao et al. Langmuir, 32, 5078-5084, 2016; Zhong, Cao et al. JCPB, 116, 3249-3263, 2012[13,28]]. Component III (~3625 cm^{-1}) can be mainly attributed to water molecules interacting with only one anion [Wei et al. JCPB, 123, 4766-4775, 2019[48]]. In that case both OH groups might be doubly H-bonded with the same anion or, more likely, the formation of asymmetric configurations should be considered ($O\cdots H-O-H\cdots A^-$). In these configurations, one OH group interacts with one anion while the other OH is H-bonded to a second water molecule. Finally, component I (~ 3475 cm^{-1}) can be assigned to water-water H-bonds involving water molecules already associated to the anion [Fazio et al. *J. Raman Spectrosc.* **39**, 233–237 (2008); Masaki et al. J. Phys. Chem. B, 114, 6323-6331, 2010[26,44]]. Considering their spectral location, these water-water H-bonds are still significantly weaker than those formed, in average, in neat water, whose Raman spectrum presents two main components at ~3200 and ~3400 cm^{-1} assigned to tetrahedral (ice-like) structures and more distorted configurations, respectively [Paolantoni, et al. J. Phys. Chem. A 113, 15100 (2009)[42]]. Reasonably, water-water H-bonds described by component I are weaker than those of pure water due to the reduction of (tetrahedral) ordering and cooperative effects caused by the anion on proximal water (to be verified). Nevertheless, in the Raman spectra of Figure 1 (a) the persistence of a spectral signature at around 3200 cm^{-1} (labelled with *), due to the ice-like component of bulk water, can be inferred even for the more concentrated [BMIM][BF_4] solutions. Based on the relative intensity between normalized SC and solution spectra, a rough estimate of the fraction of hydration water into the system can be attempted. As a result, about 80 % of bulk water is found to be still present in the x_{IL}=0.12 solution. Thus, the three components observed in the SC spectra (Fig 1 (c)) specifically account for the fraction of water molecules located in the "interface" between IL clusters and the percolating bulk-like water network [Zhong, Cao et al. JCPB, 116, 3249-3263, 2012[28]]. From the fraction of hydration water, a quantitative estimate of the (minimum) number of perturbed water molecules per solute [Fega et al, Applied Spectroscopy, 66, 3, 2012; Wu et al, Angew. Chem. Int .Ed, 57,15133 –15137, 2018[36,49]] - here referred to as apparent hydration number (N_h) - can be also obtained. As evidenced in Figure 3, in diluted conditions (at least) about 3 water molecules per anion are structurally affected. Moreover, the average N_h for [BMIM][BF_4] (blue pentagons) decreases with x_{IL} indicating the occurrence of anion clustering in the explored concentration range. This is in line with Fig 2(c), where a relative increase of component II is observed at higher x_{IL} values, confirming that the formation of $A^-\cdots H-O-H\cdots A^-$ structures is favored, with respect to $O\cdots H-O-H\cdots A^-$ ones, at higher IL concentrations. Thus, Raman findings reveal an overall decrease of the anion exposition to water upon increasing of x_{IL}, pointing out the presence of IL aggregates and their modulation (i.e. size and/or distribution) within $0.02<x_{IL}<0.12$. Since the

[BMIM][BF_4] is expected to fully dissociate only at at x_{IL} < 0.02 [Katayanagi, Koga et al. JPCB, 108, 19451-19457, 2004[15]], the observed modifications would involve ion aggregates. The occurrence of changes in aggregation properties of the [BMIM][BF_4]/water mixtures agrees with previous MD simulations [Zhong, Cao et al. JCPB, 116, 3249-3263, 2012; Chang J. Phys. Chem. B 2021, 125, 1227−1240[28,50]]. Here we demonstrate that these changes can be detected as subtle modulations of the interactions experienced by the interfacial water. Evaluating the CH stretching trends of the groups belonging to the imidazole ring (signals at 3050-3200 cm^{-1}) we do not observe any relevant shift within 0.02<x_{IL}<0.12, in line with previous IR investigations [Jeon et al. JPCB, 112, 923-928][27], suggesting that the strong anion-cation interactions (ion-pairs) remain rather unperturbed. Moreover, the relatively strong concentration dependence, reported for the CH_3 and CH_2 stretching bands at 2800-3000 cm^{-1} of the butyl moiety [Jeon et al. JPCB, 112, 923-928[27]] is not confirmed by our data, which instead suggest that also the local environment around the hydrophobic portions of the cations is not strongly affected by the aggregation process. These data are consistent with the presence ion aggregates, stabilized by cation-cation hydrophobic contacts and anion-water interactions, forming nano-domains dispersed in the water medium, possibly with micellar-like character [Gao et al. Langmuir, 32, 5078-5084, 2016[13]]. These aggregates and their hydration properties should play a role in determining the concentration fluctuation features evidenced by SANS experiments.

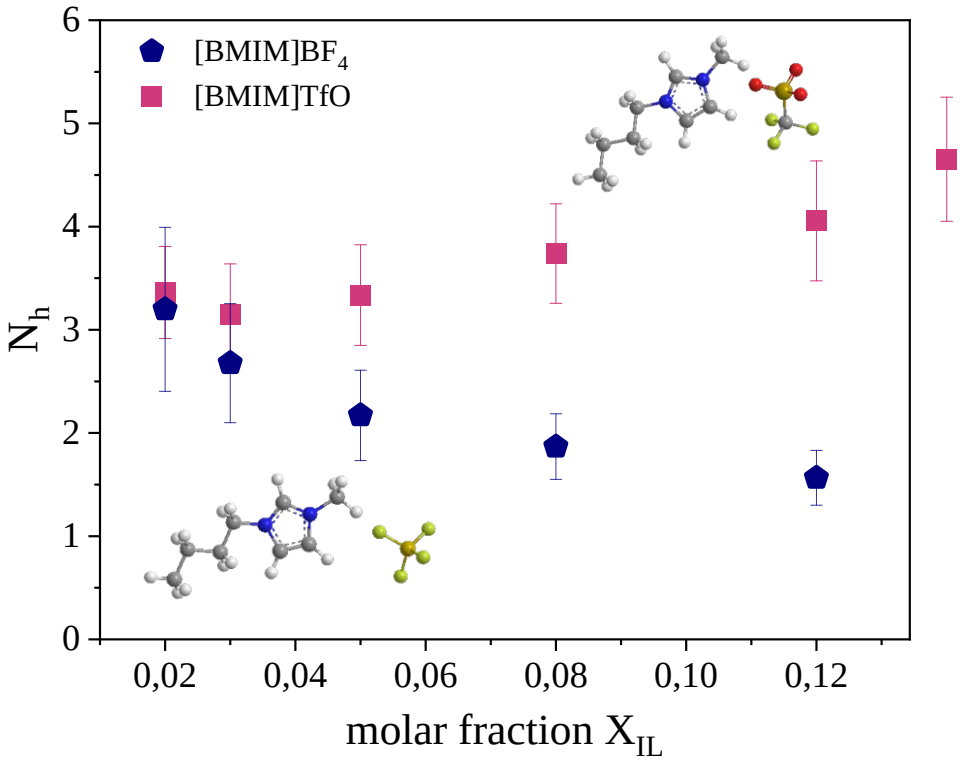

Figure 3: Apparent hydration number N_h (number of water molecules perturbed by solute) derived for aqueous solutions of [BMIM][BF_4] (blue pentagons) and [BMIM][TFO] (violet squares).

A significantly different scenario emerged from the analysis of the SC spectra of [BMIM][TfO] (Fig 1 (d)). SC spectra show one single component positioned at about 3500 cm^{-1} that can be assigned [Cammarata et al. PCCP, 3, 5292-5200, 2001[31]] to the symmetric stretching ν_1 of water molecules interacting with two different TfO anions ($A^-\cdots H-O-H\cdots A^-$). Anyhow, the assignment to water molecules H-bonded to a single TfO anion cannot be excluded. The position of the band indicates that the strength of water-anion

H-bonds increases significantly on going from BF_4 to TfO. Based on a frequency-energy empirical correlation, [Cammarata et al. PCCP, 3, 5292-5200, 2001[31]] the water-TfO H-bonding energy of about 16 kJ/mol can be estimated. As reported in Figure 3, an apparent hydration number of about 3.5 is found, indicating that, in diluted conditions, the number water-anion H-bonds formed by TfO and BF_4 are similar. Nevertheless, for the [BMIM][TfO] mixtures, neither the number of perturbed water molecules nor the corresponding SC spectral distribution depend on concentration. Thus, in this case, IL clustering processes were not evidenced, and the anion solvation is rather unperturbed within the $0.02 < x_{IL} < 0.12$ range. This agrees with the reported propensity of TfO to form strong H-bonds with both water and cation [Saihara et al, JPCB, 119,1611-1622, 2015[51]]. A recent study on [Emim][TfO]/water mixtures, further emphasized that TfO tends to interact strongly with water, while maintaining a persistent anion-cation interaction, even in high diluted conditions, for the particular stability of the hydrated ion-pair dimers [Singh et al. JPCB, 123, 4004-4016, 2019[52]].
Considering the CH stretching signals, also in this case, no meaningful modifications were detected in the $0.02 < x_{IL} < 0.12$ range, in general agreement line with previous studies on the related [EMIM][TfO] compound. [Singh et al. JPCB, 123, 4004-4016, 2019[52]] Thus, together with literature results, our Raman analysis in the water-rich domain of [BMIM][TfO] mixtures points out the existence of persistent IL-water adducts, as reflected by cation CH stretching bands and anion hydration features. As a result, the amount of "interfacial water" in this system grows up significantly with x_{IL}, and only ~ 45 % of bulk water is estimated to exist at x_{IL}=0.12. Likely, the stronger water-anion H-bonds contribute to reduce aggregate growth with x_{IL} more efficiently in the [BMIM][TfO] mixtures compared to [BMIM][BF_4]. Thus, the two systems clearly exhibit a different tendency to aggregation related to the nature of the anion. The replacement of BF_4 with TfO modifies the properties of the interfacial water and its amount.
In summary, three important aspects emerge from the analysis of the UV Raman data: i) the IL-water interactions are modulated by the specific structural features and H-bond properties of the anions, with the BF_4 acting as a weaker H-bond acceptor compared to TfO; ii) BF_4 hydration is more sensitive to IL concentration compared to TfO, evidencing modifications on aggregation features; iii) strictly connected to ii) is the key concept of "interfacial water" - between IL and water domains - playing a role in differentiating the molecular organization of the two IL/water mixtures and their concentration dependence. These features should be kept in mind when analyzing the patterns of density inhomogeneities from SANS experiments.

The mesoscopic viewpoint: SANS experiments. SANS profiles obtained for [BMIM][BF_4]/D_2O and [BMIM][TfO]/D_2O solutions in the $0.02 < x_{IL} < 0.12$ range at 25°C are shown, as an example, in Figure 4.

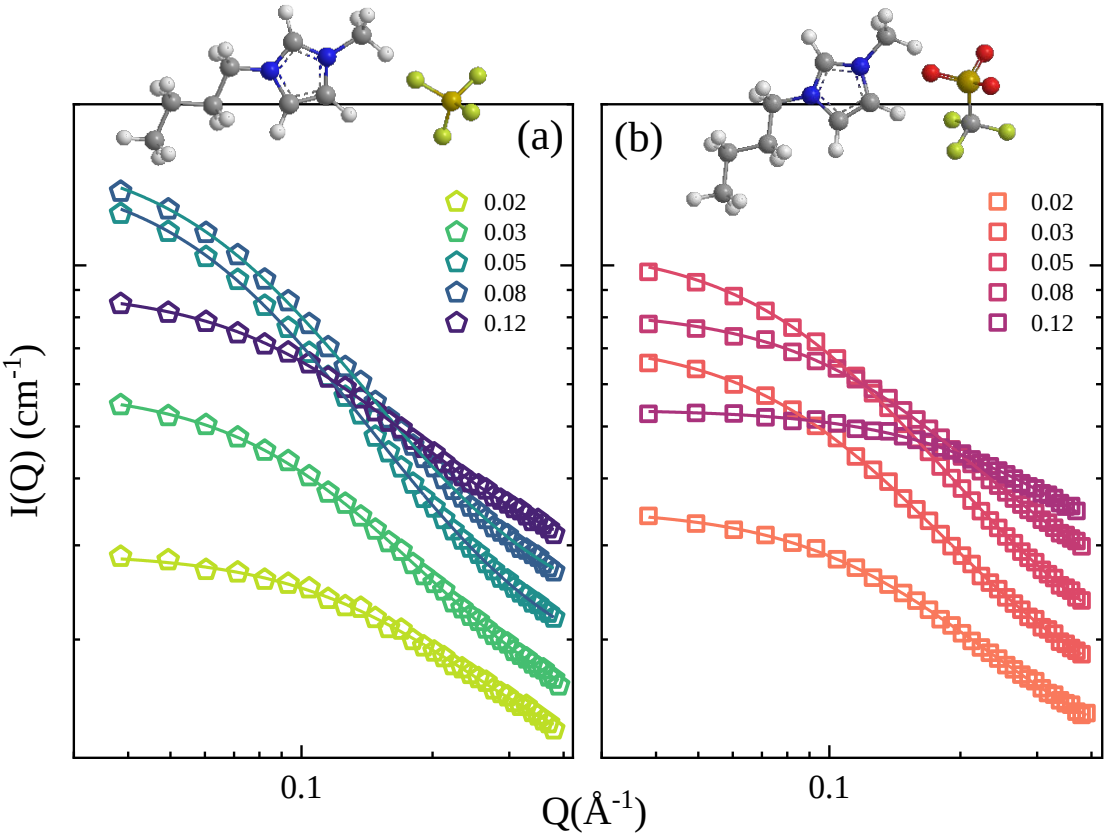

Figure 4. SANS patterns collected on [BMIM][BF4] (a) and [BMIM][TfO] (b) aqueous solutions at various molar fraction values and at temperature of 25 °C. The continuous lines are fitting of the experimental data obtained by using eq 1 (see text for details).

The scattering curves were analyzed by using the Ornstein-Zernike form for statistical concentration fluctuations given by the equation:

$$I(q) = \frac{I_0}{1+q^2\xi^2} + Bg \qquad (1)$$

where I_0 represents the coherent forward scattering intensity, ξ is the short-range correlation length, which measures the decay of density-density correlations and *Bg* represents a constant background. This latter term takes into account the contribution of the incoherent scattering from hydrogen and deuterium atoms and it can be expressed as:

$$Bg = a \cdot v_f + b(1 - v_f)$$

where a and b are two constants while v_f represents the IL volume fraction, considering the number of hydrogen and deuterium atoms. The Bg contribution does not depend on temperature, being v_f constant at a fixed molar fraction. The measurements were collected as function of temperature and a global curve-fitting was performed with Bg as a common parameter. This allowed us to reduce the total number of free parameters in Eq. 1 during the fitting procedure. Figure 4 clearly points out that the experimental SANS curves are well reproduced by the Ornstein-Zernike function for all the examined

concentrations. This suggests that the overall molecular distribution is that expected when strong concentration fluctuations occur.

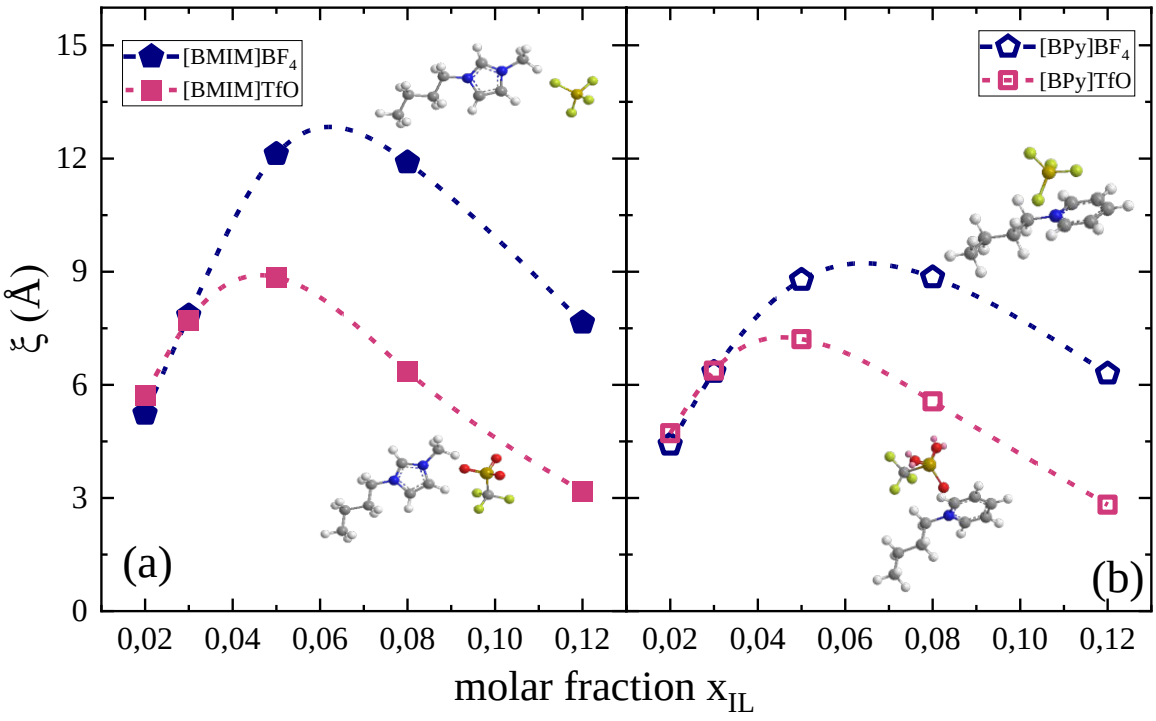

Figure 5. Concentration dependence of correlation lengths ξ estimated for [BMIM][BF_4] and [BMIM][TfO] aqueous solutions (a) and for [BPy][BF_4]and [BPy][TfO] aqueous solutions (b) at 25 °C. The dashed lines are guides for eyes.

The Ornstein-Zernike correlation lengths estimated as a function of x_{IL} for the two imidazolium-based systems and for two pyridinium homologues, [BPy][BF_4] and [BPy][TfO], are shown in Figures 5(a) and 5(b), respectively. In this respect, it is interesting to consider how density fluctuations may be sensitive to the replacement of both anion and cation.

In all the cases, the curves show a maximum at a characteristic IL mole fraction, confirming the density inhomogeneity in water environments. The correlation length ξ for [BMIM][BF_4]/water mixtures is ~ 13 Å, the absolute maximum found in this study. In particular, the trend observed for [BMIM][BF_4]/D_2O mixtures is consistent with that reported by Almásy et al. [Almásy et al. J. Phys. Chem. B, 112, 8, 2008[16]] in previous SANS experiments at T = 25 °C, validating the whole data set. The correlation length in the case of [BMIM][TfO] is lower, ~9 Å, indicating a lower degree of micro- heterogeneities, in accordance with its more homogeneous solvation features observed by UV-Raman data. Interestingly, the same pattern of ξ is observed for [BPy][BF_4]/D_2O and [BPy][TfO]/D_2O, respectively, thus confirming the pivotal role of the anions in driving the solvation/aggregation pathways at these dilution regimes.

The SANS results can be related to those obtained from the analysis of SC-UV Raman spectra. Based on these latter, the properties of interfacial water in [BMIM][BF_4] samples show a higher concentration dependence than [BMIM][TfO] ones, reflecting enhanced modulations of aggregation features. At the same time, the SANS analysis suggests that [BMIM][BF_4] aqueous mixtures are also more heterogenous at mesoscopic scales and relatively more affected by concentration changes. Likely, the presence of more stable TfO-water structures, involving relatively stronger H-bonding interactions than BF_4-water ones, might be relevant in determining the different behavior. In this respect, while hydrophobic

interactions triggered by the cations are likely responsible for the occurrence of strong concentration fluctuations and for the general trends depicted in Figure 5, the enhanced IL aggregation, evidenced by Raman data for the [BMIM][BF_4]/water mixtures (Figure 3), might increase the overall extent of micro-heterogeneity. As a matter of fact, for both mixtures the correlation length is similar at low IL concentration, while it increases faster with x_{IL} for the [BMIM][BF_4] mixture that clearly shows signatures of ion aggregation (Figures 2 and 3). From a different perspective, it also possible to infer that the interfacial water itself might regulate (directly or indirectly) the extent of microheterogeneity of the mixtures. To notice that the amount of bulk water is different in the two systems just because of the different aggregation propensity of the two anions (Figure 3). A schematic comparative representation of the molecular distribution in the two mixtures - involving IL aggregates, bulk and interfacial water - as derived by analysis of UV Raman and SANS experiments, is pictured in Figure 6. Here it is emphasized that the [BMIM][BF_4] mixture is relatively more heterogenous, encompassing larger IL aggregates and a lower amount of interfacial water.

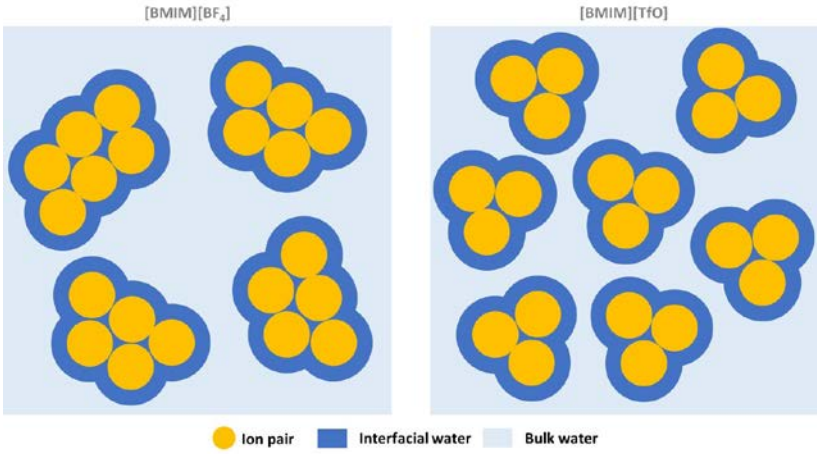

Figure 6. Schematic representation of the molecular distribution (involving IL aggregates, bulk and interfacial water) expected in a [BMIM][BF_4]/water mixture (left) and [BMIM][TfO]/water mixture (right), when compared at the same mole fraction. According to experimental SANS and Raman data, the [BMIM][BF_4] mixture is relatively more heterogenous, with larger ion aggregates and smaller amount of interfacial water.

The temperature dependence of the Ornstein-Zernike correlation length estimated for the four selected ILs as function of x_{IL} is shown in Figure 7.

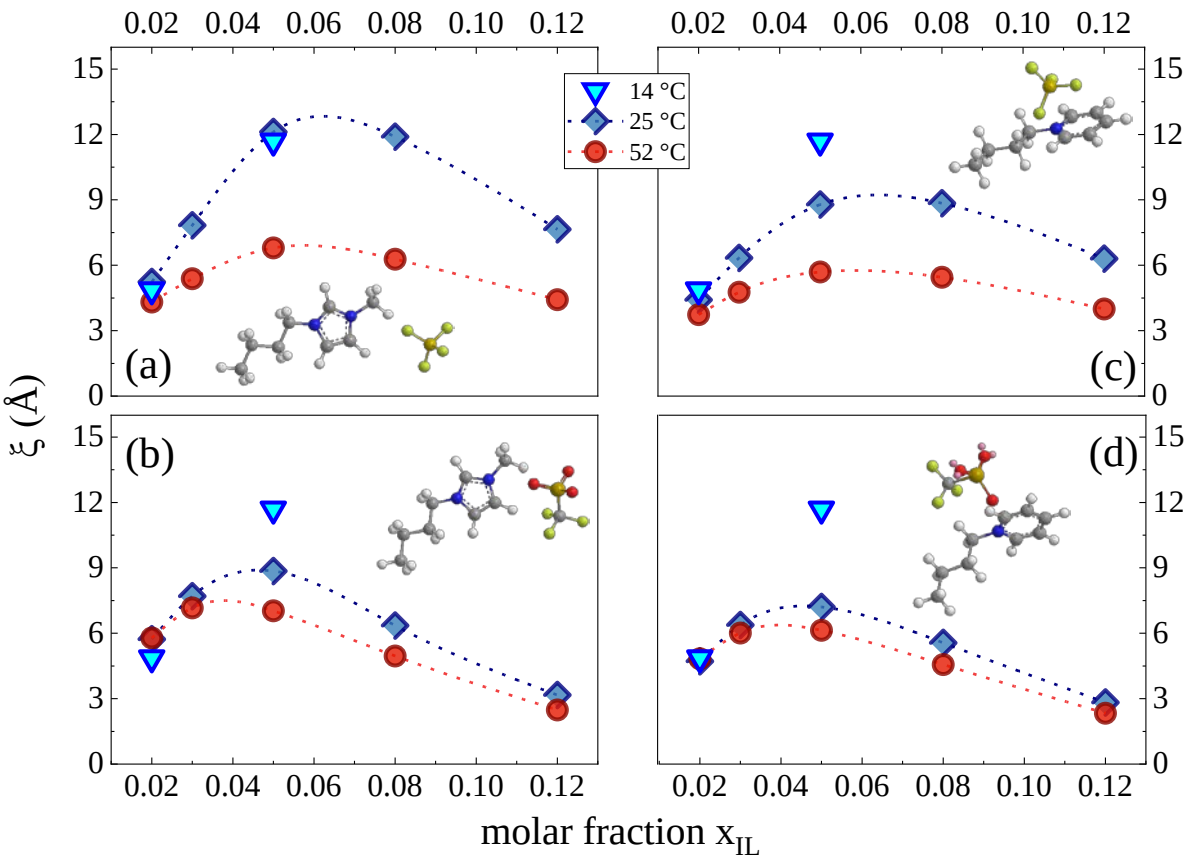

Figure 7. Concentration dependence of correlation lengths ξ estimated for [BMIM][BF_4] (a), [BMIM][TfO] (b), [BPy][BF_4] (c) and [BPy][TfO] (d) aqueous solutions at different temperatures. The dashed lines are guides for eyes.

The plots of Figure 7(a) show a marked decrease of ξ at 50~~2~~ °C compared to 25 °C in the case of [BMIM][BF_4] solutions. A similar trend is observed in Figure 6(c) for the IL sharing the same anion [BPy][BF_4], although at a lesser extent. Conversely, the plots of Figure 6(b) and Figure 6(d) show small variations of the correlation length on passing from 25 to 50~~2~~ °C. The temperature patterns support the interpretation here proposed: the stronger water-anion H-bonds observed in the case of TfO containing ILs lead to a persistent hydration shell that likely prevents changes of the IL aggregation features (or their mutual interactions), even doubling the temperature.

Conclusions

In this work, a direct spectral subtraction procedure on the OH stretching band of UV Raman spectrum made it possible to extract the solute-correlated (SC) spectrum, which highlights spectral contributions due to hydration water in the aqueous solutions of ILs.[34,35] These SC-UV Raman spectra were determined for aqueous solutions of two related ionic liquids, [BMIM][BF_4] and [BMIM][TfO], to characterize, for the first time, the local structuring of the *interfacial water* in micro-heterogeneous samples, encompassing IL aggregates and bulk water domains. SC-UV Raman data uncovered the different hydration features of [BMIM][BF_4] and [BMIM][TfO] specifically attributed to anion-water interactions. The existence of IL aggregates and their concentration dependence clearly emerge for [BMIM][BF_4]. The data are generally consistent with the idea that in the water-rich regime ILs, similarly to surfactant, tend to associate through their hydrophobic portions. Yet, specific features arise due to

the nature of the anion. In this respect, SC-UV Raman spectra evidence how ionic aggregates enlarge at increasing IL concentrations in the case of [BMIM][BF_4], which forms relatively weak H-bonds with water. On the other hand, stronger water-anion H-bonds are observed for [BMIM][TfO], leading to a more persistent hydration shell that likely prevents changes of the IL aggregates (or their mutual interactions). Overall, SC-UV Raman spectroscopy allowed us to obtain the spectral distribution of interfacial water in prototypical ILs. This is a step forward to achieve a deep view of the hydrogen bonding interactions that establish between interfacial water and ionic liquid in the water-rich regime.

SANS experiments, also extended to [BPy][BF_4] and [BPy][TfO] aqueous solutions, evidenced the occurrence of significant concentration fluctuations and micro-inhomogeneity for all the IL/water mixtures in the water-rich domain. These were mainly ascribed to the IL aggregation, likely induced by the hydrophobic parts of the cation. Nevertheless, the major variations of concentration fluctuations observed for [BMIM][BF_4] (and [BPy][BF_4]) compared to the TfO analogues led to the idea that the weaker anion-water interactions, favoring IL aggregation, contribute in enhancing the micro-heterogenous character of the mixture.

In conclusion, UV Raman and SANS experiments allowed us to probe at a microscopic and mesoscopic scale, respectively, aggregation properties of IL mixtures in a water-rich environment and how concentration-induced changes of the anion hydration (*interfacial water*) relate to modifications on the micro-heterogeneity (concentration fluctuations) in IL/water mixtures.

Acknowledgements

The authors acknowledge the CERIC-ERIC Consortium for access to experimental facilities and financial support (proposal number 20177079 and 20187101). The authors would like to thank Dr. A. Gessini of the IUVS beamline at Elettra for the technical support during UVRR measurements.

Bibliography

(1) Urahata, S. M.; Ribeiro, M. C. C. Structure of Ionic Liquids of 1-Alkyl-3-Methylimidazolium Cations: A Systematic Computer Simulation Study. J. Chem. Phys. 2004, 120 (4), 1855–1863. https://doi.org/10.1063/1.1635356.

(2) Wang, Y.; Voth, G. A. Unique Spatial Heterogeneity in Ionic Liquids. J. Am. Chem. Soc. 2005, 127 (35), 12192–12193. https://doi.org/10.1021/ja053796g.

(3) Canongia Lopes, J. N. A.; Pádua, A. A. H. Nanostructural Organization in Ionic Liquids. J. Phys. Chem. B 2006, 110 (7), 3330–3335. https://doi.org/10.1021/jp056006y.

(4) Triolo, A.; Russina, O.; Bleif, H.-J.; Di Cola, E. Nanoscale Segregation in Room Temperature Ionic Liquids †. J. Phys. Chem. B 2007, 111 (18), 4641–4644. https://doi.org/10.1021/jp067705t.

(5) Russina, O.; Triolo, A.; Gontrani, L.; Caminiti, R. Mesoscopic Structural Heterogeneities in Room-Temperature Ionic Liquids. J. Phys. Chem. Lett. 2012, 3 (1), 27–33. https://doi.org/10.1021/jz201349z.

(6) Triolo, A.; Russina, O.; Fazio, B.; Appetecchi, G. B.; Carewska, M.; Passerini, S. Nanoscale Organization in Piperidinium-Based Room Temperature Ionic Liquids. J. Chem. Phys. 2009, 130 (16), 164521. https://doi.org/10.1063/1.3119977.

(7) Wang, Y.-L.; Li, B.; Sarman, S.; Mocci, F.; Lu, Z.-Y.; Yuan, J.; Laaksonen, A.; Fayer, M. D. Microstructural and Dynamical Heterogeneities in Ionic Liquids. Chem. Rev. 2020, 120 (13), 5798–5877. https://doi.org/10.1021/acs.chemrev.9b00693.

(8) Kohno, Y.; Ohno, H. Ionic Liquid/Water Mixtures: From Hostility to Conciliation. Chem. Commun. 2012, 48 (57), 7119. https://doi.org/10.1039/c2cc31638b.

(9) Azov, V. A.; Egorova, K. S.; Seitkalieva, M. M.; Kashin, A. S.; Ananikov, V. P. “Solvent-in-Salt” Systems for Design of New Materials in Chemistry, Biology and Energy Research. Chem. Soc. Rev. 2018, 47 (4), 1250–1284. https://doi.org/10.1039/C7CS00547D.

(10) Ma, C.; Laaksonen, A.; Liu, C.; Lu, X.; Ji, X. The Peculiar Effect of Water on Ionic Liquids and Deep Eutectic Solvents. Chem. Soc. Rev. 2018, 47 (23), 8685–8720. https://doi.org/10.1039/C8CS00325D.

(11) Moreno, M.; Castiglione, F.; Mele, A.; Pasqui, C.; Raos, G. Interaction of Water with the Model Ionic Liquid [Bmim][BF 4]: Molecular Dynamics Simulations and Comparison with NMR Data. J. Phys. Chem. B 2008, 112 (26), 7826–7836. https://doi.org/10.1021/jp800383g.

(12) Nordness, O.; Brennecke, J. F. Ion Dissociation in Ionic Liquids and Ionic Liquid Solutions. Chem. Rev. 2020, 120 (23), 12873–12902. https://doi.org/10.1021/acs.chemrev.0c00373.

(13) Gao, J.; Wagner, N. J. Water Nanocluster Formation in the Ionic Liquid 1-Butyl-3-Methylimidazolium Tetrafluoroborate ([C 4 Mim][BF 4])–D 2 O Mixtures. Langmuir 2016, 32 (20), 5078–5084. https://doi.org/10.1021/acs.langmuir.6b00494.

(14) Bowers, J.; Butts, C. P.; Martin, P. J.; Vergara-Gutierrez, M. C.; Heenan, R. K. Aggregation Behavior of Aqueous Solutions of Ionic Liquids. Langmuir 2004, 20 (6), 2191–2198. https://doi.org/10.1021/la035940m.

(15) Katayanagi, H.; Nishikawa, K.; Shimozaki, H.; Miki, K.; Westh, P.; Koga, Y. Mixing Schemes in Ionic Liquid−H 2 O Systems: A Thermodynamic Study. J. Phys. Chem. B 2004, 108 (50), 19451–19457. https://doi.org/10.1021/jp0477607.

(16) Almásy, L.; Turmine, M.; Perera, A. Structure of Aqueous Solutions of Ionic Liquid 1-Butyl-3-Methylimidazolium Tetrafluoroborate by Small-Angle Neutron Scattering. J. Phys. Chem. B 2008, 112 (8), 2382–2387. https://doi.org/10.1021/jp076185e.

(17) Perera, A.; Sokolić, F.; Almásy, L.; Westh, P.; Koga, Y. On the Evaluation of the Kirkwood-Buff Integrals of Aqueous Acetone Mixtures. J. Chem. Phys. 2005, 123 (2), 024503. https://doi.org/10.1063/1.1953535.

(18) Almásy, L.; Len, A.; Szekely, N. K.; Plestil, J. Solute aggregation in dilute aqueous solutions of tetramethylurea. Fluid Phase Equilib. 2007, 257 (1), 114-119. https:// 10.1016/j.fluid.2007.05.016.

(19) Shimomura, T.; Fujii, K.; Takamuku, T. Effects of the Alkyl-Chain Length on the Mixing State of Imidazolium-Based Ionic Liquid–Methanol Solutions. Phys. Chem. Chem. Phys. 2010, 12 (38), 12316. https://doi.org/10.1039/c0cp00614a.

(20) Kusano, T.; Fujii, K.; Tabata, M.; Shibayama, M. Small-Angle Neutron Scattering Study on Aggregation of 1-Alkyl-3-Methylimidazolium Based Ionic Liquids in Aqueous Solution. J. Solution Chem. 2013, 42 (10), 1888–1901. https://doi.org/10.1007/s10953-013-0080-0.

(21) Abe, H.; Takekiyo, T.; Shigemi, M.; Yoshimura, Y.; Tsuge, S.; Hanasaki, T.; Ohishi, K.; Takata, S.; Suzuki, J. Direct Evidence of Confined Water in Room-Temperature Ionic Liquids by Complementary Use of Small-Angle X-Ray and Neutron Scattering. J. Phys. Chem. Lett. 2014, 5 (7), 1175–1180. https://doi.org/10.1021/jz500299z.

(22) Sastry, N. V.; Vaghela, N. M.; Macwan, P. M.; Soni, S. S.; Aswal, V. K.; Gibaud, A. Aggregation Behavior of Pyridinium Based Ionic Liquids in Water – Surface Tension, 1H NMR Chemical Shifts, SANS and SAXS Measurements. J. Colloid Interface Sci. 2012, 371 (1), 52–61. https://doi.org/10.1016/j.jcis.2011.12.077.

(23) McDaniel, J. G.; Verma, A. On the Miscibility and Immiscibility of Ionic Liquids and Water. J. Phys. Chem. B 2019, 123 (25), 5343–5356. https://doi.org/10.1021/acs.jpcb.9b02187.

(24) Verma, A.; Stoppelman, J. P.; McDaniel, J. G. Tuning Water Networks via Ionic Liquid/Water Mixtures. IJMS 2020, 21 (2), 403. https://doi.org/10.3390/ijms21020403.

(25) Paschoal, V. H.; Faria, L. F. O.; Ribeiro, M. C. C. Vibrational Spectroscopy of Ionic Liquids. Chem. Rev. 2017, 117 (10), 7053–7112. https://doi.org/10.1021/acs.chemrev.6b00461.

(26) Fazio, B.; Triolo, A.; Di Marco, G. Local Organization of Water and Its Effect on the Structural Heterogeneities in Room-Temperature Ionic Liquid/H 2 O Mixtures: Local Organization of Water in Ionic Liquid/H 2 O Mixtures. J. Raman Spectrosc. 2008, 39 (2), 233–237. https://doi.org/10.1002/jrs.1825.

(27) Jeon, Y.; Sung, J.; Seo, C.; Lim, H.; Cheong, H.; Kang, M.; Moon, B.; Ouchi, Y.; Kim, D. Structures of Ionic Liquids with Different Anions Studied by Infrared Vibration Spectroscopy. J. Phys. Chem. B 2008, 112 (15), 4735–4740. https://doi.org/10.1021/jp7120752.

(28) Zhong, X.; Fan, Z.; Liu, Z.; Cao, D. Local Structure Evolution and Its Connection to Thermodynamic and Transport Properties of 1-Butyl-3-Methylimidazolium Tetrafluoroborate and Water Mixtures by Molecular Dynamics Simulations. J. Phys. Chem. B 2012, 116 (10), 3249–3263. https://doi.org/10.1021/jp3001543.

(29) Zheng, Y.-Z.; Zhou, Y.; Deng, G.; Guo, R.; Chen, D.-F. A Combination of FTIR and DFT to Study the Microscopic Structure and Hydrogen-Bonding Interaction Properties of the [BMIM][BF4] and Water. Spectrochim. Acta A Mol. Biomol. Spectrosc. 2020, 226, 117624. https://doi.org/10.1016/j.saa.2019.117624.

(30) Wang, N.-N.; Zhang, Q.-G.; Wu, F.-G.; Li, Q.-Z.; Yu, Z.-W. Hydrogen Bonding Interactions between a Representative Pyridinium-Based Ionic Liquid [BuPy][BF4] and Water/Dimethyl Sulfoxide. J. Phys. Chem. B 2010, 114 (26), 8689–8700. https://doi.org/10.1021/jp103438q.

(31) Cammarata, L.; Kazarian, S. G.; Salter, P. A.; Welton, T. Molecular States of Water in Room Temperature Ionic Liquids Phys. Chem. Chem. Phys. 2001, 3 (23), 5192–5200. https://doi.org/10.1039/b106900d.

(32) Köddermann, T.; Wertz, C.; Heintz, A.; Ludwig, R. The Association of Water in Ionic Liquids: A Reliable Measure of Polarity. Angew. Chem. Int. Ed. 2006, 45 (22), 3697–3702. https://doi.org/10.1002/anie.200504471.

(33) Yoshimura, Y.; Mori, T.; Kaneko, K.; Nogami, K.; Takekiyo, T.; Masuda, Y.; Shimizu, A. Confirmation of Local Water Structure Confined in Ionic Liquids Using H/D Exchange. J. Mol. Liq. 2019, 286, 110874. https://doi.org/10.1016/j.molliq.2019.04.151.

(34) Perera, P.; Wyche, M.; Loethen, Y.; Ben-Amotz, D. Solute-Induced Perturbations of Solvent-Shell Molecules Observed Using Multivariate Raman Curve Resolution. J. Am. Chem. Soc. 2008, 130 (14), 4576–4577. https://doi.org/10.1021/ja077333h.

(35) Ben-Amotz, D. Hydration-Shell Vibrational Spectroscopy. J. Am. Chem. Soc. 2019, 141 (27), 10569–10580. https://doi.org/10.1021/jacs.9b02742.

(36) Fega, K. R.; Wilcox, A. S.; Ben-Amotz, D. Application of Raman Multivariate Curve Resolution to Solvation-Shell Spectroscopy. Appl Spectrosc 2012, 66 (3), 282–288. https://doi.org/10.1366/11-06442.

(37) Davis, J. G.; Gierszal, K. P.; Wang, P.; Ben-Amotz, D. Water Structural Transformation at Molecular Hydrophobic Interfaces. Nature 2012, 491 (7425), 582–585. https://doi.org/10.1038/nature11570

(38) Wilcox, D. S.; Rankin, B. M.; Ben-Amotz, D. Distinguishing Aggregation from Random Mixing in Aqueous T-Butyl Alcohol Solutions. Faraday Discuss. 2013, 167, 177. https://doi.org/10.1039/c3fd00086a.

(39) Putz, A-M.; Almasy, L.; Horvath, Z. E.; Trif, L. Butyl-Methyl-Pyridinium Tetrafluoroborate Confined in Mesoporous Silica Xerogels: Thermal Behaviour and Matrix-Template Interaction. Materials 2021, 14, 4918. https://doi.org/10.3390/ma14174918

(40) Rossi, B.; Bottari, C.; Catalini, S.; Gessini, A.; D'Amico, F.; Masciovecchio, C. Synchrotron based UV Resonant Raman scattering for material science, Molecular and Laser Spectroscopy, ed. V. P. Gupta and Y. Ozaki, Elsevier, 2020, ch. 13, vol. 2. https://doi.org/110.1016/B978-0-12-818870-5.00013-7.

(41) Gallina, M. E.; Sassi, P.; Paolantoni, M.; Morresi, A.; Cataliotti, R. S. Vibrational Analysis of Molecular Interactions in Aqueous Glucose Solutions. Temperature and Concentration Effects. J. Phys. Chem. B 2006, 110 (17), 8856–8864. https://doi.org/10.1021/jp056213y.

(42) Paolantoni, M.; Lago, N. F.; Albertí, M.; Laganà, A. Tetrahedral Ordering in Water: Raman Profiles and Their Temperature Dependence. J. Phys. Chem. A 2009, 113 (52), 15100–15105. https://doi.org/10.1021/jp9052083.

(43) Bottari, C.; Comez, L.; Paolantoni, M.; Corezzi, S.; D'Amico, F.; Gessini, A.; Masciovecchio, C.; Rossi, B. Hydration Properties and Water Structure in Aqueous Solutions of Native and Modified Cyclodextrins by UV Raman and Brillouin Scattering. J Raman Spectrosc 2018, 49 (6), 1076–1085. https://doi.org/10.1002/jrs.5372.

(44) Masaki, T.; Nishikawa, K.; Shirota, H. Microscopic Study of Ionic Liquid−H 2 O Systems: Alkyl-Group Dependence of 1-Alkyl-3-Methylimidazolium Cation. J. Phys. Chem. B 2010, 114 (19), 6323–6331. https://doi.org/10.1021/jp1017967.

(45) López-Pastor, M.; Ayora-Cañada, M. J.; Valcárcel, M.; Lendl, B. Association of Methanol and Water in Ionic Liquids Elucidated by Infrared Spectroscopy Using Two-Dimensional Correlation and Multivariate Curve Resolution. J. Phys. Chem. B 2006, 110 (22), 10896–10902. https://doi.org/10.1021/jp057398b.

(46) Schröder, C.; Hunger, J.; Stoppa, A.; Buchner, R.; Steinhauser, O. On the Collective Network of Ionic Liquid/Water Mixtures. II. Decomposition and Interpretation of Dielectric Spectra. The Journal of Chemical Physics 2008, 129 (18), 184501. https://doi.org/10.1063/1.3002563.

(47) Danten, Y.; Cabaço, M. I.; Besnard, M. Interaction of Water Highly Diluted in 1-Alkyl-3-Methyl Imidazolium Ionic Liquids with the PF 6 − and BF 4 − Anions. J. Phys. Chem. A 2009, 113 (12), 2873–2889. https://doi.org/10.1021/jp8108368.

(48) Wei, Q.; Zhang, M.; Zhou, D.; Li, X.; Bian, H.; Fang, Y. Ultrafast Hydrogen Bond Exchanging between Water and Anions in Concentrated Ionic Liquid Aqueous Solutions. J. Phys. Chem. B 2019, 123 (22), 4766–4775. https://doi.org/10.1021/acs.jpcb.9b03504.

(49) Wu, X.; Lu, W.; Streacker, L. M.; Ashbaugh, H. S.; Ben-Amotz, D. Methane Hydration-Shell Structure and Fragility. Angew. Chem. Int. Ed. 2018, 57 (46), 15133–15137. https://doi.org/10.1002/anie.201809372.

(50) Chang, T.-M.; Billeck, S. E. Structure, Molecular Interactions, and Dynamics of Aqueous [BMIM][BF4] Mixtures: A Molecular Dynamics Study. J. Phys. Chem. B 2021, 125 (4), 1227–1240. https://doi.org/10.1021/acs.jpcb.0c09731.

(51) Saihara, K.; Yoshimura, Y.; Ohta, S.; Shimizu, A. Properties of Water Confined in Ionic Liquids. Sci Rep 2015, 5 (1), 10619. https://doi.org/10.1038/srep10619.

(52) Singh, D. K.; Donfack, P.; Rathke, B.; Kiefer, J.; Materny, A. Interplay of Different Moieties in the Binary System 1-Ethyl-3-Methylimidazolium Trifluoromethanesulfonate/Water Studied by Raman Spectroscopy and Density Functional Theory Calculations. J. Phys. Chem. B 2019, 123 (18), 4004–4016. https://doi.org/10.1021/acs.jpcb.9b00066.